# Method of Evaluating Delayed Fracture Susceptibility of Tempered Martensitic Steel Showing Quasi-Cleavage Fracture

YU MATSUMOTO and KENICHI TAKAI

The difference in the hydrogen charging methods, immersion in a NH$_4$SCN aqueous solution, and cathodic electrolysis in a NaOH aqueous solution, did not affect the hydrogen state present in the steel, but it did affect the surface state of the specimens through corrosion, causing fracture strength to fluctuate in tensile testes. As for stress application method, the fracture strength at lower crosshead speeds in tensile tests was consistent with that found for hydrogen precharging prior to stress application in CLTs as long as hydrogen charging was conducted by cathodic electrolysis. However, the fracture strength obtained with concurrent hydrogen charging without precharging prior to stress application in CLTs was higher than that with hydrogen precharging prior to stress application in CLTs regardless of the same hydrogen content. In other words, delayed fracture susceptibility was affected by the order of hydrogen charging and stress application for quasi-cleavage fracture associated with local plastic deformation, *i.e.*, dislocation motion. Therefore, by taking into account the cathodic electrolysis in the NaOH solution, the low crosshead speed and the order of hydrogen charging and stress application, the fracture strength in CLTs, and tensile tests coincided with respect to quasi-cleavage fracture even though the stress application methods were different.

## I. INTRODUCTION

A method for evaluating delayed fracture susceptibility has to be established for applying high-strength steels more widely in order to assess the safety of such steels in actual environments and develop steels with lower delayed fracture susceptibility. A number of evaluation methods have been proposed so far.[1–5] They can be categorized as providing either a relative or an absolute evaluation. The former type of evaluation can determine only the comparative merits of different kinds of steels, whereas the latter type can estimate the lifetime of steels in actual environments and assess whether they can be used or not. Both relative and absolute evaluation methods require hydrogen charging in a laboratory and the application of stress for accelerating delayed fracture, which can occur in a few months to a couple of decades in an actual environment.[6]

Widely used methods of hydrogen charging include immersion in HCl or NH$_4$SCN aqueous solution, cathodic electrolysis, and exposure in a high-pressure hydrogen gas atmosphere. Regardless of the type of hydrogen charging method used, the states of hydrogen present in steels are identical under the same charging temperature and hydrogen content.[7,8] However, immersion methods change the surface states of steels[8] and cause the blunting of notches[6] due to corrosion and dissolution, which affect fracture strength in delayed fracture tests. Hydrogen charging and stress application procedures differ among researchers. Some researchers start hydrogen charging followed by the simultaneous application of constant stress,[5] *i.e.*, hydrogen is absorbed after almost all mobile dislocations have slipped and piled up; other researchers precharge hydrogen prior to starting stress application,[9] *i.e.*, almost all mobile dislocations slip in the presence of hydrogen. Although this difference may affect fracture strength, its effect has not been well understood.

As for stress application, both static stress and dynamic stress have been widely applied. Examples of static stress application include a constant load test (CLT)[5,9,10] and a U-bending test.[3] Examples of dynamic stress applied in tensile tests[4,11,12] at constant strain rates include a slow strain rate tensile test (SSRT)[4,11] and a conventional strain rate tensile test,[1,12] which have been proposed as methods for evaluating delayed fracture susceptibility. Ensuring the consistency of fracture strength between static and dynamic methods is a critical issue. Terasaki and Tsuzaki have reported that CLT results coincide with those of SSRTs,[13] while another study has reported inconsistencies.[14] Since the experimental conditions such as materials, hydrogen charging methods, stress application methods, and experimental procedures used in previous studies differed among research

YU MATSUMOTO is with the Graduate School of Science and Technology, Sophia University, 7-1 Kioi-cho, Chiyoda-ku, Tokyo, 102-8554, Japan, and also with Nippon Steel & Sumitomo Metal Corporation, Chiba, Japan. KENICHI TAKAI is with the Department of Engineering and Applied Science, Faculty of Science and Technology, Sophia University, 7-1 Kioi-cho, Chiyoda-ku, Tokyo, 102-8554, Japan. Contact e-mail: takai@me.sophia.ac.jp

organizations, the essential reasons for the differences among the reports remain unclear. Clarifying the conditions consistent between SSRTs and CLTs would be valuable in discussing the results reported by various research organizations in the future.

In addition to hydrogen charging and stress application methods, the fracture modes of evaluated steels can also affect the results of delayed fracture tests. In general, steels with high strength and high delayed fracture susceptibility tend to exhibit intergranular fracture due to hydrogen; steels with relatively low strength and low delayed fracture susceptibility show quasi-cleavage fracture, which propagates transgranularly through lath boundaries.[15–17] Three-point bending tests have shown that quasi-cleavage cracks initiate at notch tips where local strain is maximum, whereas intergranular fracture initiates slightly inside notch tips where local stress is maximum.[18,19] These results suggest that strain-controlled fracture leads to the quasi-cleavage mode and that stress-controlled fracture leads to the intergranular mode. In other words, quasi-cleavage and intergranular fractures seem to be caused by different fracture mechanisms. Assuming that the mechanisms are different, we have to discuss the evaluation methods separately between the two fracture modes since the effects of the test conditions on the delayed fracture results probably differ between the modes.

In the present study, tempered martensitic steel containing a high silicon content of 1.67 mass pct, which exhibits mainly quasi-cleavage fracture due to hydrogen, was employed as test specimens. The effects of hydrogen charging and stress application methods on delayed fracture susceptibility were investigated. With regard to hydrogen charging, immersion in a NH$_4$SCN aqueous solution and cathodic electrolysis were compared. For the stress application methods, fracture strengths in CLTs as one type of static test and in tensile tests as one type of dynamic test were compared. The effect of precharging, *i.e.*, the effect of the order of hydrogen charging and stress application on fracture strength, was investigated.

## II. EXPERIMENTAL

### A. *Materials*

Tempered martensitic steel was prepared for use as test specimens. Table I shows the chemical composition of the tested steel. Round bar specimens with a diameter of 5.0 mm were induction quenched and tempered, as shown in Figure 1. The tensile strength and a 0.2 pct proof stress were 1446 and 1421 MPa, respectively. The precipitated carbide particles were very fine because of

**Table I. Chemical Compositions of Tested Steel (Mass Percent)**

| C | Si | Mn | P | S | Cu | Ti |
|------|------|------|-------|-------|------|------|
| 0.32 | 1.67 | 0.75 | 0.014 | 0.005 | 0.01 | 0.02 |

the high silicon content of 1.67 mass pct. Hence, the fracture mode under hydrogen charging was not intergranular, but mainly quasi-cleavage.[14] For delayed fracture susceptibility tests, the specimens were notched circumferentially after induction heating, as shown in Figure 2. The depth of the notch was determined as 0.4 mm on the basis of the depth data of pits formed by atmospheric corrosion.

### B. *Hydrogen Charging and Hydrogen Analysis*

The specimens were charged with hydrogen by immersion and cathodic electrolysis methods. Prior to hydrogen charging, the specimen surface was polished with #800 emery paper to remove the oxidized scale formed during heat treatment. For the immersion method, the specimens were immersed in a 7 mass pct NH$_4$SCN aqueous solution kept at a temperature of 303 K (30 °C) for 72 hours. For the cathodic electrolysis method, the specimens were charged with hydrogen at a current density of 8 A m$^{-2}$ in a 0.1 N NaOH aqueous solution kept at 303 K (30 °C) and containing a NH$_4$SCN additive of 3 g L$^{-1}$. The charging time was determined as 72 hours so as to reach an equilibrium hydrogen concentration at both the surface and center of the specimens. These charging conditions provided an equilibrium hydrogen concentration of approximately 1 mass ppm in the steel specimens.

The hydrogen content and state were analyzed by thermal desorption analysis (TDA) using a gas chromatograph at a heating rate of 100 K h$^{-1}$ in the temperature range from room temperature to 573 K (300 °C). A standard gas mixture of Ar + 50 vol. ppm of H$_2$ was used for calibration of the hydrogen concentration. Before TDA, the specimens were polished with #800 emery paper to remove corrosion products so that the surface was uniform.

### C. *Delayed Fracture Susceptibility*

Tensile tests and CLTs were employed as the evaluation methods for delayed fracture susceptibility. Prior to the tensile tests, the specimens were precharged with hydrogen by the immersion and cathodic electrolysis methods for 72 hours under the conditions described in Section II–B. Hydrogen charging was conducted concurrently during the tensile tests in order to prevent hydrogen evolution, and the tensile tests continued until fracture occurred. The crosshead speeds used in the tensile tests varied from 0.05 to 20 mm min$^{-1}$. Nominal stress ($\sigma$) was defined as $\sigma = F/A_{min}$, where $F$ is the tensile load and $A_{min}$ is the initial net cross-sectional area of the notch in the specimen. In the CLTs, the specimens were precharged with hydrogen for 72 hours under the same charging conditions as in the tensile tests, followed by the application of constant tensile stress. Hydrogen charging was continued during the application of stress in order to prevent hydrogen evolution. In contrast, CLTs without precharging, *i.e.*, stress application and hydrogen charging began at the same time, were also conducted to ascertain the effect of hydrogen precharging on fracture strength. More
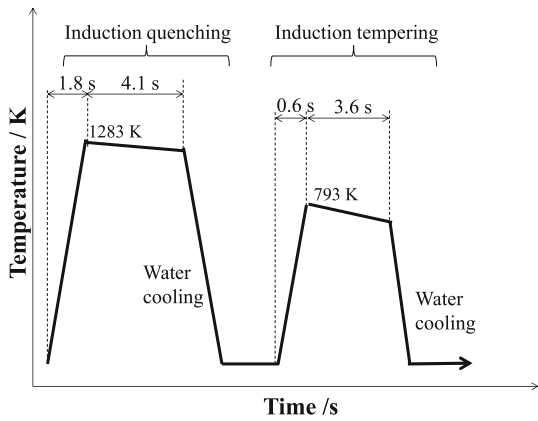
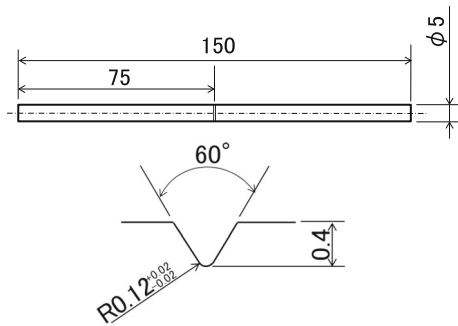Fig. 1—Schematic diagram of heat treatment cycle of tested steel.



Fig. 2—Geometry and dimensions of a notched specimen for tensile testing.
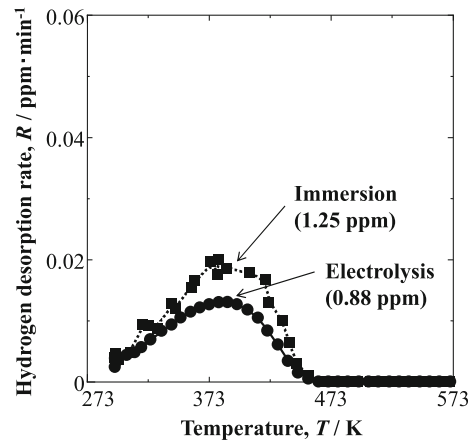


Fig. 3—Thermal desorption profiles and hydrogen contents of specimens after hydrogen charging by immersion or cathodic electrolysis. Immersion took place in a 7 mass pct NH₄SCN solution at 303 K (30 °C) for 72 h. Cathodic electrolysis was performed at a current density of 8 A m$^{-2}$ in a 0.1 N NaOH solution kept at a temperature of 303 K (30 °C) and containing a NH₄SCN additive of 3 g L$^{-1}$.
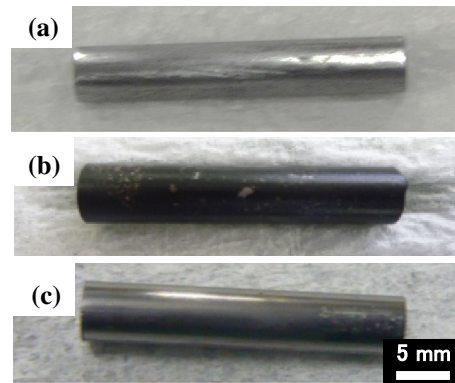


Fig. 4—Photographs of specimen surface: (a) before hydrogen charging, (b) after immersion in a 7 mass pct NH₄SCN solution at 303 K (30 °C) for 72 h, and (c) after cathodic electrolysis at a current density of 8 A m$^{-2}$ in a 0.1 N NaOH solution kept at a temperature of 303 K (30 °C) and containing a NH₄SCN additive of 3 g L$^{-1}$.

precisely, hydrogen charging was begun a few seconds after starting to apply stress. Constant nominal stresses from 295 to 1595 MPa were applied in the CLTs, and the time to fracture was recorded. The delayed fracture strength, assumed to correspond to delayed fracture susceptibility, was defined as the maximum stress without fracture within 100 hours. To determine the maximum stress without fracture, CLTs were conducted at least three times under applied stress and it was affirmed that all the specimens did not fracture.

## III. RESULTS

### A. States of Hydrogen Present in Specimens and Surface States of Specimens

Hydrogen desorption profiles and hydrogen contents of the specimens charged with hydrogen by the immersion and cathodic electrolysis methods are shown in Figure 3. The peak temperatures at 383 K (110 °C) and desorption temperature ranges of hydrogen were the same for both methods. This result indicates that the states of hydrogen present in the specimens were identical even though different hydrogen charging methods were employed, which is consistent with the previous papers.[7,8] The hydrogen contents charged by the immersion and cathodic electrolysis methods under the conditions used were measured to be 1.3 and 0.9 mass

ppm, respectively. The scattering of the hydrogen concentration under the same charging condition was ±0.15 mass ppm.

Figure 4 shows the photographs of specimen surfaces: (a) before hydrogen charging, (b) after immersion, and (c) after cathodic electrolysis. A metallic luster was observed on the specimen surfaces both (a) before hydrogen charging and (c) after cathodic electrolysis. In contrast, the specimen surface (b) after immersion lost its luster and was covered with a black corrosion product that was found by analysis to consist of Fe, O, and S.[8] Scanning electron micrographs of specimen surfaces at the notches (a) before hydrogen charging, (b) after immersion, and (c) after cathodic electrolysis are shown in Figure 5.

Macroscopically, the curvatures of the notches seem to be the same among the three specimens. Microscopically, however, circumferential tool marks were
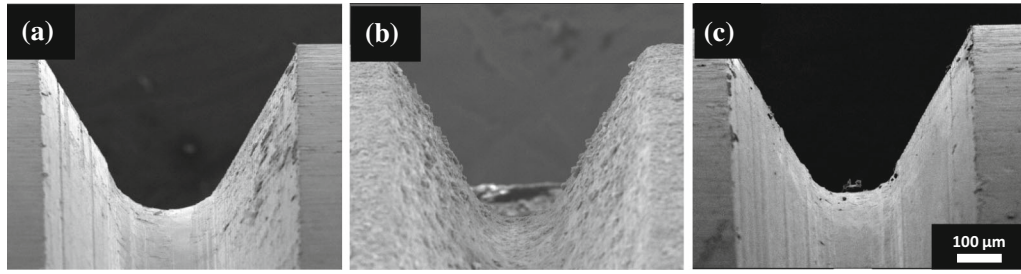
Fig. 5—Scanning electron micrographs in the vicinity of the notches of specimens: (*a*) before hydrogen charging, (*b*) after immersion in a 7 mass pct NH$_4$SCN solution at 303 K (30 °C) for 72 h, and (*c*) after cathodic electrolysis at a current density of 8 A m$^{-2}$ in a 0.1 N NaOH solution kept at a temperature of 303 K (30 °C) and containing a NH$_4$SCN additive of 3 g L$^{-1}$.

observed as the vertical lines in Figure 5 on the notch surfaces (a) before hydrogen charging and (c) after cathodic electrolysis. This indicates that cathodic electrolysis in a NaOH aqueous solution does not change the surface state. In contrast, the tool marks disappeared on the notch surface (b) after immersion, and small bumps formed on the surface owing to the dissolution of iron.

In summary, the curvatures of notches did not change macroscopically during hydrogen charging by the two methods of immersion and cathodic electrolysis. However, the immersion method caused microscopic changes in the specimen surface state owing to the dissolution of iron. Hence, delayed fracture tests using the immersion method can evaluate not only the effect of hydrogen but also the effect of the change in the surface state, whereas the cathodic electrolysis method in a NaOH aqueous solution enables only an evaluation of the simple effect of hydrogen since this method does not affect the specimen surface.

### B. Tensile Test with Precharging

Stress–displacement curves obtained in tensile tests of specimens notched circumferentially with/without hydrogen charging at various crosshead speeds are shown in Figure 6. Hydrogen precharging was carried out for 72 hours followed by a tensile test concurrently with hydrogen charging using the cathodic electrolysis method at a current density of 8 A m$^{-2}$ in a 0.1 N NaOH solution kept at a temperature of 303 K (30 °C) and containing a NH$_4$SCN additive of 3 g L$^{-1}$. The maximum stress was defined as the fracture strength. The effect of hydrogen on the fracture strength and elongation was the smallest at a high crosshead speed of 20 mm min$^{-1}$ and the fracture strength of specimens charged with hydrogen decreased with decreasing crosshead speed.

Figure 7 shows the relationship between the fracture strength with/without hydrogen charging and the crosshead speed in tensile tests of the notched specimens. The crosshead speeds were varied from 0.005 to 20 mm min$^{-1}$. The fracture strengths of uncharged notched specimens remained constant over various crosshead speeds, whereas the fracture strength of specimens charged by cathodic electrolysis decreased with decreasing crosshead speed in the range from 20 to 0.02 mm min$^{-1}$. At a crosshead speed of 0.005 mm min$^{-1}$, there are two plots ($n$ = 2). When a
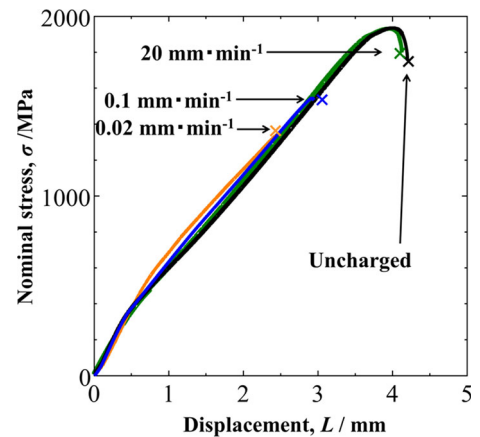


Fig. 6—Stress–displacement curves in tensile testing of notched specimens at various crosshead speeds. Hydrogen precharging was conducted by cathodic electrolysis at a current density of 8 A m$^{-2}$ in a 0.1 N NaOH solution kept at a temperature of 303 K (30 °C) and containing a NH$_4$SCN additive of 3 g L$^{-1}$.
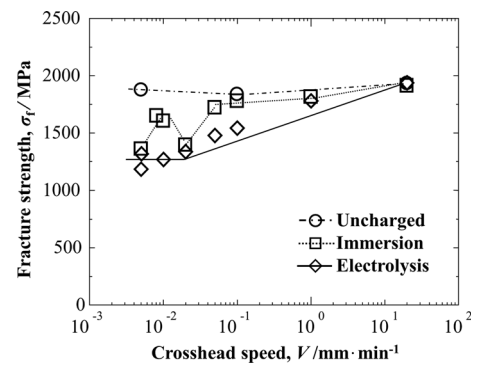


Fig. 7—Relationship between fracture strength and crosshead speed in tensile testing of notched specimens. Hydrogen charging was conducted by immersion in a 7 mass pct NH$_4$SCN or by cathodic electrolysis at a current density of 8 A m$^{-2}$ in a 0.1 N NaOH solution kept at a temperature of 303 K (30 °C) and containing a NH$_4$SCN additive of 3 g L$^{-1}$.

line is connected between the average of those two fracture strengths and the fracture strength at a crosshead speed of 0.01 mm min$^{-1}$, the line is horizontal. Hence, the fracture strength remained constant below a crosshead speed of 0.02 mm min$^{-1}$. When the immersion method was

employed, a similar tendency was observed. However, the fracture strength fluctuated and the relationship between the fracture strength and the crosshead speed showed less correlation. Hence, fracture strength was not necessarily the same between the two hydrogen charging methods even though the specimens, hydrogen content, and hydrogen state were almost the same.

Scanning electron micrographs of the specimen surfaces fractured in tensile tests during hydrogen charging by (a) immersion and (b) cathodic electrolysis are shown in Figure 8. The specimens in both (a) and (b) showed mainly quasi-cleavage fracture, which included a small part of intergranular fracture. There was no difference between the two fracture surfaces regardless of the difference in hydrogen charging methods.

### C. Constant Load Test with Precharging

The fracture strength and fractography obtained in CLTs were compared with those obtained in tensile tests. In this section, only cathodic electrolysis was employed since it did not affect the surface state of the specimens and allowed a comparison of the net effect of the stress application methods. The hydrogen charging conditions in the CLTs were the same as in the tensile tests. Figure 9 shows the relationship between the applied constant stress and the time to fracture in CLTs with hydrogen precharging for 72 hours. Some specimens did not fracture, even though constant stress of 1595 MPa was applied, while others soon fractured at applied stress of 1377 MPa. The delayed fracture strength at which fracture did not occur within 100 hours was found to be 1160 MPa. This stress level was nearly equal to the fracture strength of 1184 MPa that was obtained in tensile tests conducted at lower crosshead speeds below 0.02 mm min$^{-1}$, as shown in Figure 7.

Figure 10 shows the macroscopic fracture surfaces of the hydrogen-charged specimens after CLTs or tensile tests, as observed by SEM. The hatched area was a brittle-like fracture surface, i.e., quasi-cleavage (QC) or intergranular (IG). The other area was a ductile fracture surface, i.e., dimple pattern. The brittle area was very small on the fracture surface after tensile tests conducted at a high crosshead speed of 20 mm min$^{-1}$. This is consistent with the observation that fracture strength did not decrease at a high crosshead speed of 20 mm min$^{-1}$ even though specimens had the same hydrogen content. As the crosshead speed decreased, the brittle area increased. The distribution of the brittle area in the fracture surface after CLTs under 1377 MPa was similar to that after tensile tests at a low crosshead speed of 0.02 mm min$^{-1}$. The fracture strengths were almost the same for the specimen at 0.02 mm min$^{-1}$ and that of CLT as shown in Figures 7 and 9. These similarities indicate that the fracture process was the same between SSRTs and CLTs, although the stress application modes were different.

Microscopic fracture surfaces after CLTs and tensile tests at a low crosshead speed of 0.02 mm min$^{-1}$ are shown in Figure 11, as observed by SEM. Both fracture surfaces showed mainly quasi-cleavage fracture, which partially included intergranular fracture.

Thus, stress application methods with precharging did not affect the fracture strength and fracture surface when the material and hydrogen content were the same, and cathodic electrolysis, which does not affect the surface state, was employed for hydrogen charging.

### D. Constant Load Test Without Precharging

Figure 12 shows the relationship between the applied constant stress and the time to fracture in CLTs when hydrogen precharging was not conducted, i.e., hydrogen charging and constant stress application commenced at the same time. More precisely, hydrogen charging was begun a few seconds after starting to apply stress. Even when tensile stress of 1595 MPa was applied, the specimens charged with hydrogen did not fracture even after more than 100 hours for both hydrogen charging methods. Since no fracture occurred, the delayed fracture strength could not be determined. However, it was not less than 1595 MPa, which was at least 435 MPa higher than that (1160 MPa) in CLTs with hydrogen precharging (Figure 9). The minimum fracture strength in tensile tests, $\sigma_{\text{preH-SSRT}}$, (Figure 7), the delayed fracture strength of precharged specimens in CLTs, $\sigma_{\text{PreH-CLT}}$, (Figure 9) and the delayed fracture strength in CLTs without precharging, $\sigma_{\text{CLT}}$, (Figure 12) are summarized in Figure 13.
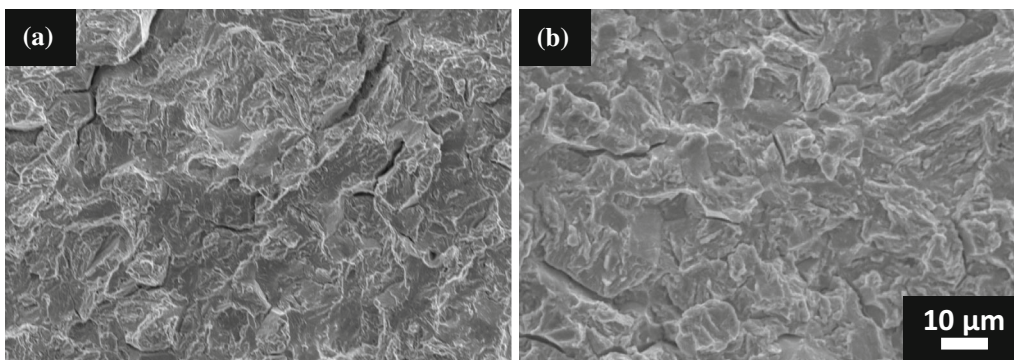


Fig. 8—Microscopic fracture surfaces in the vicinity of the notch root after tensile testing at a crosshead speed of 0.02 mm min$^{-1}$. Hydrogen charging was conducted by (a) immersion and (b) cathodic electrolysis.

In conclusion, the fracture strength in CLTs and the fracture strength in tensile tests at lower crosshead speeds were almost the same under the following conditions: hydrogen precharging and also charging during stress application were conducted by cathodic electrolysis. It will be noted that hydrogen precharging had a substantial effect on delayed fracture strength in CLTs. CLTs without hydrogen precharging resulted in much larger delayed fracture strength than in CLTs and tensile tests with hydrogen precharging.

## IV. DISCUSSION

### A. *Effect of Hydrogen Charging Methods on Delayed Fracture Evaluation*

The effects of the hydrogen charging methods on the results obtained in the delayed fracture tests are discussed here. The fracture strengths obtained with the immersion method were more unstable than those obtained with the cathodic electrolysis method, as shown in Figure 7. Consequently, fracture strengths are not necessarily identical between the two hydrogen charging methods. The fracture strengths obtained with
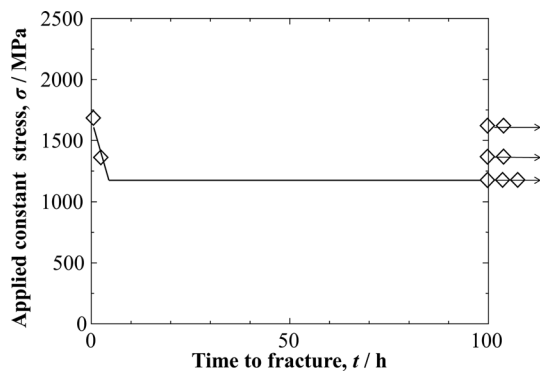


Fig. 9—Relationship between applied stress and time to fracture in CLTs with hydrogen precharging for 72 h. Hydrogen charging was conducted by cathodic electrolysis at a current density of 8 A m$^{-2}$ in a 0.1 N NaOH solution kept at a temperature of 303 K (30 °C) and containing a NH$_4$SCN additive of 3 g L$^{-1}$.

the immersion method tended to be the same or slightly higher than those obtained with the cathodic electrolysis method. The difference in fracture strengths between the two methods is not ascribed to the hydrogen states and contents since the hydrogen state was identical and the hydrogen contents obtained with the immersion method were the same or higher than those obtained with the cathodic electrolysis method, as described in Section III–A. The NH$_4$SCN aqueous solution used in this work dissolves iron and forms a corrosion product on the specimen surface. Though the amount of dissolution was not large enough to change the shape of the notches, it was large enough to eliminate the tool marks and surface roughness, as shown in Figure 5. Though the corrosion rate was not measured in this study, the weight loss of steels in a 0.1 mass pct NH$_4$SCN aqueous solution at a temperature of 298 K (25 °C)[7] and in a 20 mass pct NH$_4$SCN aqueous solution at a temperature of 323 K (50 °C)[20] was reported. The weight loss of steels in a 20 mass pct NH$_4$SCN aqueous solution at a temperature of 323 K (50 °C) was almost 0.001 g cm$^{-2}$ after 20 hours,[20] which was smaller than that in an aqueous solution of HCl of 3.0 in pH at a temperature of 298 K (25 °C)[7] by nearly one order of magnitude. In this study, the corrosion rate must be smaller than that study[7] since a 7 mass pct NH$_4$SCN aqueous solution at a temperature of 303 K (30 °C) was employed. The reduction of surface roughness probably led to increased fracture strength. The surface states probably continued to change during immersion since corrosion products cyclically form and peel off due to brittleness.[8] Thus, the unstable fracture strengths obtained with the immersion method are attributed to unstable surface states during the tensile tests, whereas the fracture strengths obtained with the cathodic electrolysis method were affected by only the hydrogen content as the surface state did not change. Accordingly, these findings reveal that the difference in hydrogen charging methods affected the results of the delayed fracture evaluation; the fracture strengths obtained with the immersion method were affected by the hydrogen content and surface state, while the fracture strengths obtained with the cathodic electrolysis method were affected only by the hydrogen content.
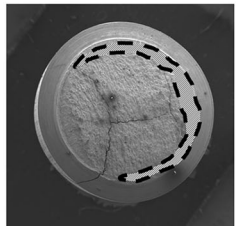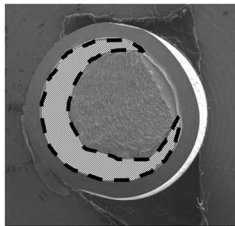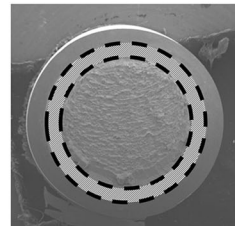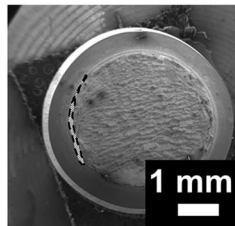


| CLT | Tensile tests | | |
|---|---|---|---|
| 1377 MPa | 0.02 mm·min$^{-1}$ | 0.1 mm·min$^{-1}$ | 20 mm·min$^{-1}$ |

Fig. 10—Macroscopic fracture surfaces after tensile testing or CLTs with hydrogen precharging for 72 h. Hydrogen charging was conducted by cathodic electrolysis. The area of QC or IG is hatched.

## B. *Effect of Stress Application Methods on Delayed Fracture Evaluation*

The effects of the stress application methods on the results of the delayed fracture tests are discussed here. For the specimens with hydrogen precharging, the fracture strength obtained in CLTs was almost identical to that in tensile tests at lower crosshead speeds below 0.02 mm min$^{-1}$, as shown in Figure 13. Terasaki and Tsuzaki[13] reported that the fracture strengths obtained in SSRTs at lower crosshead speeds below 0.005 mm min$^{-1}$ were consistent with those of CLTs. They conducted hydrogen precharging and employed a Cd coating on the specimen surfaces in order to prevent hydrogen desorption during SSRTs.

With increasing crosshead speed, however, the fracture strengths in tensile tests increased as shown in Figure 7, *i.e.*, the difference in fracture strengths between tensile tests and CLTs in Figure 9 increased, even though the same hydrogen content was charged. At the highest crosshead speed of 20 mm min$^{-1}$, in particular, the fracture strength of the hydrogen-charged specimens and that of the uncharged specimens were almost the same. In addition, the area of the brittle fracture surface decreased with increasing crosshead speed, as shown in Figure 10. Therefore, the presence of hydrogen in the specimens did not affect fracture strength under higher crosshead speeds. These results indicate that not only the presence of hydrogen but also the microscopic changes in the steel caused by the lower crosshead speeds probably played an important role in delayed fracture. The factors considered regarding the crosshead speed dependence of fracture strength are as follows:

(A)  Increment in total equilibrium hydrogen concentration caused by the longer testing time of the tensile tests.
(B)  Increment in local equilibrium hydrogen concentration at a notch tip by stress-driven diffusion.
(C)  Hydrogen transportation from external environment to fracture process zone.
(D)  Segregation of hydrogen transported by dislocations.
(E)  Formation of lattice defects enhanced by hydrogen and strain.

With regard to the possibility of factor (A), the testing time to fracture increased at lower crosshead speeds. Accordingly, the hydrogen content at the moment of fracture may have increased with decreasing crosshead speed since the tensile tests were conducted with concurrent hydrogen charging. In order to validate factor (A), the hydrogen contents after tensile tests were measured by TDA. The hydrogen contents before and after tensile tests at the lowest crosshead speed of 0.005 mm min$^{-1}$ were measured to be 0.9 and 0.8 mass ppm, respectively. The reason for no increase in the hydrogen content was probably due to the hydrogen precharging time of 72 hours, which was long enough for hydrogen to reach an equilibrium condition from the surface to the center of the specimen. Thus, the possibility of factor (A) can be omitted.

As for factor (B), a high stress concentration in the vicinity of the notch root probably caused hydrogen accumulation since elastic stress increases the chemical potential, resulting in an increment in the local equilibrium hydrogen concentration in the vicinity of the notch root. Since lower crosshead speeds provide time for stress-driven diffusion of hydrogen, fracture strength will decrease with lower crosshead speeds.[4] Hence,
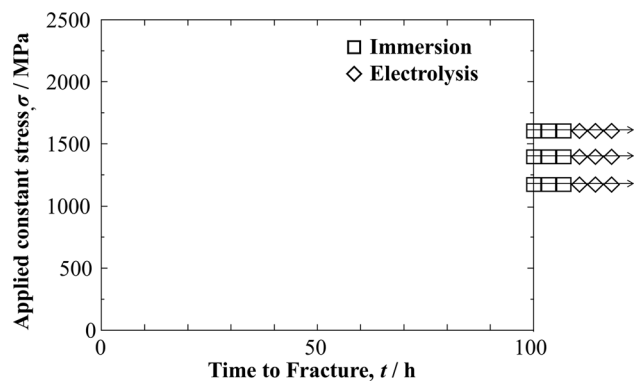


Fig. 12—Relationship between applied stress and time to fracture in CLTs without hydrogen precharging. Hydrogen was concurrently charged by immersion in a 7 mass pct NH$_4$SCN or by cathodic electrolysis at a current density of 8 A m$^{-2}$ in a 0.1 N NaOH solution kept at a temperature of 303 K (30 °C) and containing a NH$_4$SCN additive of 3 g L$^{-1}$.
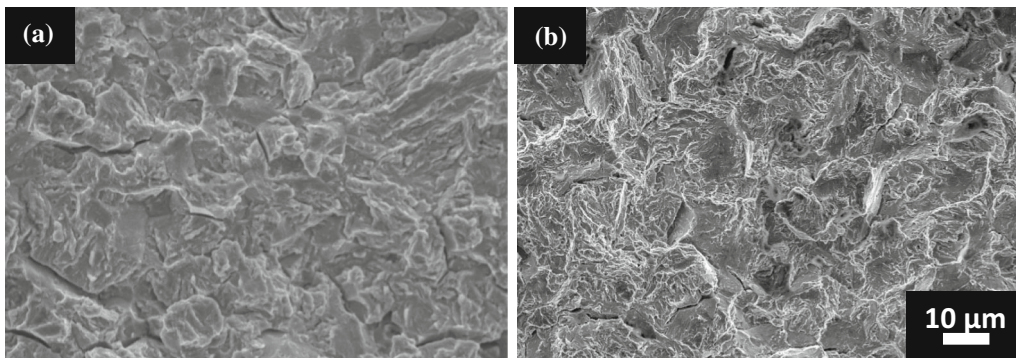


Fig. 11—Microscopic fracture surfaces in the vicinity of the notch root with hydrogen precharging for 72 h by cathodic electrolysis: (*a*) tensile testing at a crosshead speed of 0.02 mm min$^{-1}$ and (*b*) CLT.

factor (B) should be one of the major reasons in the present study. However, factor (B) is not exclusive since a crosshead speed of 1 mm min$^{-1}$ led to lower fracture strength than that at 20 mm min$^{-1}$ by approximately 130 MPa. The specimen tested at 1 mm min$^{-1}$ fractured after only 3.4 minutes, which is too short for stress-driven diffusion of hydrogen. Wang et al.[4] calculated the hydrogen concentration distribution during tensile tests of AISI 4135 steel, which has the same tensile strength of 1450 MPa as that of the steel used in this study. In the literature,[4] lower crosshead speed increased local hydrogen concentration at a notch tip by stress-driven diffusion and hydrogen concentration was constant at sufficiently low crosshead speeds since it reached equilibrium. This is consistent with the results shown in Figure 5. However, when the crosshead speed was 0.5 mm min$^{-1}$, stress-driven hydrogen diffusion hardly occurs, i.e., hydrogen was not accumulated in the vicinity of the notch root. Hence, stress-driven diffusion of hydrogen was not the only reason why fracture strength at 1.0 mm min$^{-1}$ was lower than that at 20 mm min$^{-1}$.

The possibility of factors (C), (D), and (E), therefore, needs to be discussed.

As for factor (C), hydrogen was presumably transported from the external environment to the crack-tip process zone during the tests, since the distance from the crack-tip surface to the fracture process zone was small. It has been reported that external hydrogen is more harmful than internal (precharged) hydrogen[21] in austenitic stainless steel. In this study, the specimens were not the same as those used in the previous study, but the lower crosshead speed probably provided time for the increment in hydrogen concentration at the fracture process zone due to external hydrogen absorption. That resulted in lower fracture strength at lower crosshead speeds. This factor can lower the stress level not only for crack initiation but also for crack propagation since the fracture process zone can move more slowly during crack propagation at a lower crosshead speed. This factor can lowe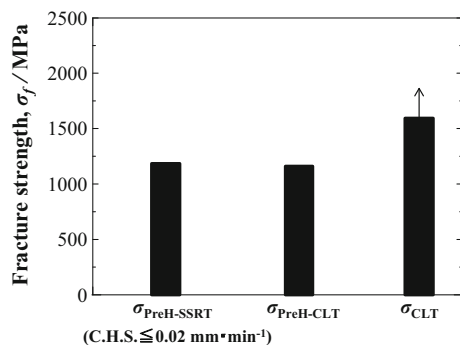r the stress level not only for crack initiation but also for crack propagation since the fracture process zone can move more slowly during crack propagation at a lower crosshead speed.

Some reports in the literature support the possibility of factors (D) and (E) with respect to the interaction between hydrogen and dislocations. It has been reported that plastic deformation under lower crosshead speeds promotes hydrogen desorption from specimens, i.e., dislocations at lower velocities transport more hydrogen to the surface of pure iron[22,23] and Ni-based alloys.[23] This transportation can be related to the crosshead speed dependence of delayed fracture susceptibility in two aspects. One is that dislocations with hydrogen pile up at grain boundaries or other obstacles, resulting in local hydrogen segregation near those obstacles such as inclusions and precipitates. The other is that the lower crosshead speed enhances the formation of lattice defects such as mono vacancies or vacancy clusters.[11,24–26] Vacancies that form during plastic deformation without the presence of hydrogen result from dislocation dynamics, such as the interaction and cutting of screw dislocations or combinations of edge dislocations with opposite characteristics located on slip planes an atomic plane distance apart, and are normally so unstable as to disappear immediately at room temperature.[27] In contrast, vacancies that form during plastic deformation in the presence of hydrogen are stabilized immediately by hydrogen since moving dislocations maintain a hydrogen atmosphere under lower strain rates. In fact, it has been shown that the formation of lattice defects by plastic deformation is enhanced by the presence of hydrogen, using lifetime measurement of positron annihilation[25,26,28,29] and analysis of hydrogen as a tracer.[24,28]

In order to validate the possibility of factors (C), (D), and (E), i.e., to omit the effect of factor (B), smooth bar specimens without any stress concentration were prepared. The gage diameter and gage length of the specimens were 3 and 20 mm, respectively. The stress–displacement curves of these smooth specimens with/without hydrogen are shown in Figure 14.

Fig. 13—Fracture strength of notched specimens in tensile testing at crosshead speeds of below 0.02 mm min$^{-1}$ ($\sigma_{\text{PreH-SSRT}}$), in CLTs with hydrogen precharging ($\sigma_{\text{PreH-CLT}}$) and in CLTs without hydrogen precharging ($\sigma_{\text{CLT}}$). Hydrogen charging was conducted by cathodic electrolysis at a current density of 8 A m$^{-2}$ in a 0.1 N NaOH solution kept at a temperature of 303 K (30 °C) and containing a NH$_4$SCN additive of 3 g L$^{-1}$.
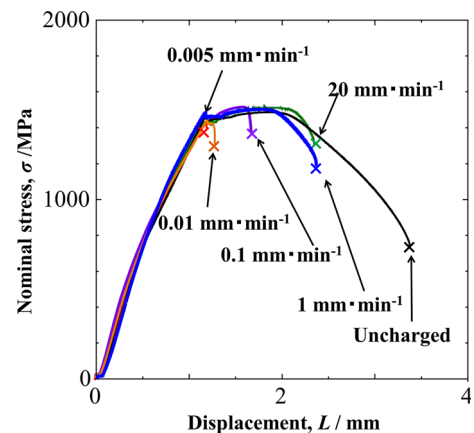
Fig. 14—Stress–displacement curves of smooth specimens in tensile testing at various crosshead speeds. Hydrogen charging was conducted by cathodic electrolysis at a current density of 20 A m$^{-2}$ in a 0.1 N NaOH solution kept at a temperature of 303 K (30 °C) and containing a NH$_4$SCN additive of 3 g L$^{-1}$.

Hydrogen precharging was conducted by cathodic electrolysis for 72 hours. The hydrogen charging temperature and solution were the same as the conditions for the notched specimens in Section II–B, while the current density was 20 A m$^{-2}$. Crosshead speeds of the tensile tests were in the range from 0.005 to 20 mm min$^{-1}$. The curve of an uncharged specimen at a crosshead speed of 20 mm min$^{-1}$ is shown in the figure as a typical stress–displacement curve. Though the total elongation decreased with decreasing crosshead speed in the range from 20 to 0.01 mm min$^{-1}$, the total elongation remained constant at crosshead speeds below 0.01 mm min$^{-1}$. These results strongly suggest that the crosshead speed dependence of ductility loss was not caused solely by stress-driven diffusion in the vicinity of the notch root since the crosshead speed dependence of ductility loss also occurred for smooth bar specimens without any stress concentration. However, hydrogen redistribution at the microscopic level probably occurs at such high hydrostatic stress fields as grain boundaries or carbides or other precipitates. The crosshead speed dependence of ductility loss of the smooth bar specimens may have been caused by redistribution of the hydrogen concentration at the microscopic level.

The fracture surfaces of the smooth specimens after the tensile tests are shown in Figure 15, as observed by SEM. The upper row shows the macroscopic fracture surface and the square areas denote the fracture origin; the lower row shows the microscopic fracture surface of the fracture origin in the square areas of the upper row. The fracture mode at the fracture origin was typical quasi-cleavage regardless of the crosshead speed. In the magnified image for 20 mm min$^{-1}$, a relatively large particle-like stuff can be seen on the right in the image. Though no analysis such as EDS was conducted, it is probably an inclusion or a precipitation based on information in the literature.[30]

Thus, the crosshead speed dependence of fracture strength was due to not only factor (B) of stress-driven diffusion, but also factor (C) for external hydrogen transportation into the fracture process zone, (D) for the dislocation transportation of hydrogen and/or factor (E) for enhanced lattice defect formation when tempered martensitic steel fractures by a quasi-cleavage mode under hydrogen charging.

## C. Effect on CLT Evaluation With/Without Hydrogen Precharging

The difference with/without hydrogen precharging affected the fracture strength in CLTs, *i.e.*, the result of delayed fracture susceptibility, as described in Section III–D. As for the effect of hydrogen precharging, the procedure for applying constant elastic stress followed by hydrogen charging implies that application of the stress has already moved and rearranged the dislocations, thereby trapping hydrogen at those sites. In contrast, the procedure for hydrogen precharging to an equilibrium concentration prior to stress application implies that the dislocations trapping hydrogen move and rearrange in the steel. The difference in effect on delayed fracture strength between with/without

hydrogen precharging is discussed below from a microscopic viewpoint.

In CLTs with hydrogen precharging for 72 hours, the time to fracture was 0.1 hour under applied stress of 1595 MPa and 1.8 hours under 1375 MPa, as shown in Figure 9. In CLTs without hydrogen precharging, on the other hand, no specimens fractured although the applied stress was as large as 1595 MPa, as shown in Figure 12. The concurrent hydrogen charging time of 100 hours during stress application was long enough to reach an equilibrium hydrogen concentration. In addition, the time of 100 hours under stress application was also long enough to reach a high local hydrogen concentration in the vicinity of the notch root, owing to the stress-driven diffusion of hydrogen. Although some small cracks may initiate during CLTs, the testing time of 100 hours should have been long enough that hydrogen also accumulated at the small crack tips without hydrogen precharging. The difference between hydrogen precharged specimens and concurrently hydrogen-charged specimens is that the former fractured after only 0.1 hour, whereas the latter did not fracture even after more than 100 hours, although both were subjected to the same stress of 1595 MPa and had the same hydrogen content. These results suggest that factor (B) of the mean or local hydrogen concentration was not the main reason for the difference in delayed fracture strength with/without hydrogen precharging. In addition, the effect of hydrogen precharging before CLTs cannot be explained by factor (C) since this factor means that precharged hydrogen is less harmful than external hydrogen during tests, which is contrary to the results of the CLTs in this study.

As for factor (D), when hydrogen precharging was conducted, the application of stress resulted in dislocation motion, hydrogen transported by dislocations and pileups at obstacles such as grain boundaries, which can cause a locally high hydrogen concentration there. When hydrogen precharging was not conducted, the application of stress also resulted in dislocation motion and pileups at grain boundaries. These pileups of dislocations can trap hydrogen and cause the segregation of hydrogen at grain boundaries. Although segregation of hydrogen should have been caused by pileups of dislocations in both specimens with/without hydrogen precharging, the delayed fracture strengths in the CLTs differed. For that reason, factor (D) can be omitted.

Only factor (E) remains to be discussed. Since mobile dislocations move microscopically even under elastic stress, the dislocations should move and lattice defects should form most actively immediately after starting the application of stress in CLTs. The reason for the lower delayed fracture strength with hydrogen precharging was probably associated with factor (E) concerning the formation of lattice defects enhanced by hydrogen and stress. In fact, it has been shown that lattice defects such as vacancy clusters are formed by hydrogen charged into the specimen under elastic constant[28] or cyclic[31] stress, using positron probe microanalyzer and tracer hydrogen as a probe of defects. In contrast, since few lattice defects would form in the absence of hydrogen immediately after starting the stress application, the delayed

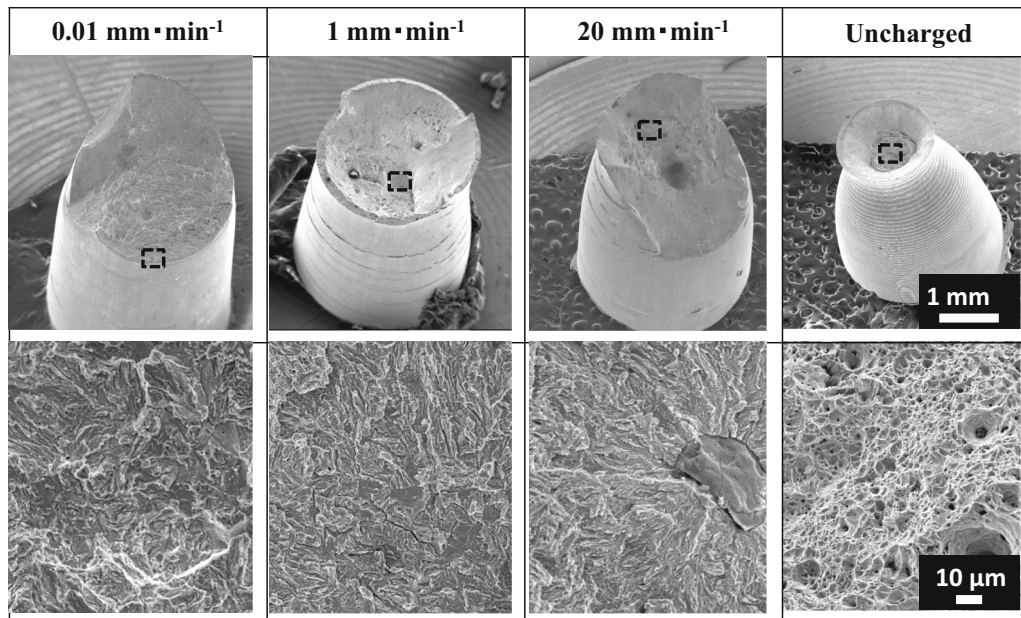| 0.01 mm·min⁻¹ | 1 mm·min⁻¹ | 20 mm·min⁻¹ | Uncharged |

Fig. 15—Macroscopic and microscopic fracture surfaces of hydrogen-charged smooth specimens after tensile testing. Hydrogen charging was conducted by cathodic electrolysis at a current density of 20 A m$^{-2}$ in a 0.1 N NaOH solution kept at a temperature of 303 K (30 °C) and containing a NH$_4$SCN additive of 3 g L$^{-1}$. The lower row shows magnified images of the crack initiation area indicated in the rectangles in the upper row.

fracture strength without hydrogen precharging was probably high.

In addition to factor (A) to (E), hydrogen-enhanced localized plasticity (HELP)[32–34] mechanism should be discussed. It has been observed by *in-situ* transmission electron microscopy that when a specimen under constant stress was charged with hydrogen, hydrogen enhanced the movement of dislocations by the HELP mechanism.[35] If HELP occurs, dislocation motion should occur for both specimens with/without precharging. However, because there was a difference in the CLT results between the precharged and non-precharged specimens, the possibility of HELP was disregarded.

These findings clearly reveal that the effect of the fracture strength obtained with/without precharging, *i.e.*, the effect of the order of hydrogen charging and stress application on fracture strength, was important for the delayed fracture evaluation. The delayed fracture strength in CLTs with hydrogen precharging was lower than that with concurrent hydrogen charging without precharging due to the interaction between hydrogen and dislocations. This suggests that the effect of hydrogen precharging on fracture strength in CLTs is attributed to lattice defect formation enhanced by hydrogen.

### D. *Method of Evaluating Susceptibility to Delayed Fracture by Quasi-Cleavage Mode*

In the present work, the factors affecting the results of delayed fracture tests were studied when the fracture mode was quasi-cleavage. Quasi-cleavage seems to be a brittle fracture macroscopically. For example, the fracture occurs without necking. However, a quasi-cleavage crack propagates along the lath boundary, which is the {110} plane[15–17] *i.e.*, the slip plane, while the cleavage fracture surface, which is known to be a low temperature brittle fracture, is along {100}. The electron diffraction pattern just beneath the fracture surface also shows the involvement of plastic deformation in hydrogen-induced quasi-cleavage.[15] Furthermore, high-density slip bands are observed just beneath the fracture surface cut with a focused ion beam, using transmission electron microscopy.[36,37] These studies indicate that quasi-cleavage is not a brittle but a ductile fracture locally. That is, movement of dislocations plays an important role in quasi-cleavage fracture. In other words, quasi-cleavage represents a large number of micro-cleavage fracture facets connected to each other by ductile fracture surfaces resembling a dimple pattern, while cleavage fracture at low temperature consists of a single fracture surface. The results in this paper, for example, the effects of the crosshead speed and hydrogen precharging on fracture strength, clearly show involvement of plastic deformation in delayed fracture. This is consistent with the literature which indicates the involvement of plastic deformation in quasi-cleavage fracture under hydrogen charging.

For the prediction of quasi-cleavage fracture, *i.e.*, fracture associated with local plastic deformation, the important conditions for consistency between CLTs and tensile tests are summarized as follows:

(1) Procedure for hydrogen precharging and stress application in CLTs and tensile tests and
(2) Low crosshead speed in tensile tests.

Even though the stress application methods in delayed fracture evaluations may differ, by taking into account the two conditions above, fracture strengths in

CLTs and tensile tests can be made to coincide. The reason is that the conditions causing the interaction between hydrogen and dislocations are considered on the basis of the hydrogen embrittlement mechanism for quasi-cleavage fracture.

In the case of actual parts such as high strength fasteners, hydrogen embrittlement evaluation with precharging may result in an overestimation of hydrogen embrittlement susceptibility. However, factor (E) is very important because, in actual environments, structural and automotive materials are often subjected to cyclic (fatigue) stress after hydrogen entry. More studies regarding the evaluation methods need to be done based on the mechanisms involved and actual environments.

In summary, the conditions for consistency between CLTs and tensile tests were found and discussed on the basis of the mechanism for delayed fracture, especially quasi-cleavage. Our next paper will describe a method for evaluating delayed fracture on the basis of an intergranular mode.

## V. CONCLUSIONS

The effects of hydrogen charging methods, stress application methods, and hydrogen precharging and stress application procedures on the results of delayed fracture susceptibility were examined for tempered martensitic steel that shows quasi-cleavage fracture due to hydrogen. The results can be summarized as follows:

(1) Hydrogen desorption profiles were almost the same for hydrogen charging by cathodic electrolysis in a NaOH aqueous solution and by immersion in a 7 mass pct $NH_4SCN$ aqueous solution at 303 K (30 °C). Hence, the hydrogen state present in the steel specimens was almost the same regardless of the different hydrogen charging methods used. However, the specimen surfaces following hydrogen charging were not the same between the different hydrogen charging methods. Immersion in a $NH_4SCN$ aqueous solution changed the surface state of the specimens due to dissolution of iron and scale formation of corrosion products, whereas cathodic electrolysis in a NaOH aqueous solution did not change the specimen surface.

(2) When hydrogen charging was conducted by immersion in a $NH_4SCN$ solution, the fracture strength of notched specimen obtained in tensile tests fluctuated and was relatively higher than that after hydrogen charging by cathodic electrolysis in a NaOH aqueous solution. Such fluctuation presumably resulted from a change in the surface state such as the dissolution of iron and the scale formation in $NH_4SCN$. The fracture strength in tensile tests was affected by not only hydrogen but also the change in the specimen surface of the notch root in the case of immersion in a $NH_4SCN$ solution for hydrogen charging. For hydrogen charging by cathodic electrolysis in a NaOH aqueous solution, the fracture strength in tensile tests was affected by only hydrogen.

(3) With higher crosshead speeds, the fracture strength in tensile tests was higher and was not consistent with that in CLTs regardless of the same hydrogen content. In contrast, with lower crosshead speeds, the fracture strength in tensile tests was consistent with that in CLTs, when hydrogen precharging was conducted to reach an equilibrium concentration prior to stress application.

(4) Regarding the effects of the hydrogen charging and stress application procedures in CLTs, the fracture strength with hydrogen precharging prior to stress application was lower than that with concurrent hydrogen charging without precharging prior to stress application. The former procedure implies that the dislocations trapping hydrogen move and rearrange in the steel. The latter procedure implies that the dislocations have already moved and rearranged prior to hydrogen charging and subsequently hydrogen was trapped at their sites. In other words, dislocation movement with hydrogen enhanced delayed fracture susceptibility, while the stabilized and rearranged dislocations had little effect on delayed fracture susceptibility, although they were trapping hydrogen. Hydrogen precharging and subsequent stress application are probably related to the formation of lattice defects. The effect of the order of hydrogen charging and stress application was important for the delayed fracture evaluation on the basis of the delayed fracture mechanism inducing quasi-cleavage fracture.

(5) Even though the stress application methods used in delayed fracture evaluations differ, by taking into account cathodic electrolysis in a NaOH solution, low crosshead speed, and the order of hydrogen charging and stress application, the fracture strengths in CLTs and tensile tests can be made to coincide for quasi-cleavage fracture.

## REFERENCES

1. Y. Hagihara: *ISIJ Int.*, 2012, vol. 52, pp. 292–97.
2. E. Akiyama: *ISIJ Int.*, 2012, vol. 52, pp. 307–15.
3. S. Takagi, Y. Toji, M. Yoshino, and K. Hasegawa: *ISIJ Int.*, 2012, vol. 52, pp. 316–22.
4. M. Wang, E. Akiyama, and K. Tsuzaki: *Scripta Mater.*, 2005, vol. 53, pp. 713–18.
5. Fédération Internationale de la Précontrainte: *Report on Prestressing Steel: 5. Stress Corrosion Cracking Resistance Test for Prestressing Tendors*, Wexham Springs, Slough, 1980, pp. 1–56.
6. S. Li, E. Akiyama, N. Uno, K. Hirai, K. Tsuzaki, and B. Zhang: *Corros. Sci.*, 2010, vol. 52, pp. 3198–3204.
7. S. Takagi and Y. Toji: *ISIJ Int.*, 2012, vol. 52, pp. 329–31.
8. T. Doshida, K. Takai, and M. Ichiba: *Corros. Eng.*, 2012, vol. 61, pp. 179–89.
9. H.H. Johnson, J.G. Morlet, and A.R. Troiano: *Trans. Metall. Soc. AIME*, 1958, vol. 212, pp. 528–36.
10. M. Wang, E. Akiyama, and K. Tsuzaki: *Corros. Sci.*, 2006, vol. 48, pp. 2189–2202.
11. T. Doshida and K. Takai: *Acta Mater.*, 2014, vol. 79, pp. 93–107.
12. Y. Hagihara, T. Shobu, N. Hisamori, H. Suzuki, K. Takai, and K. Hirai: *ISIJ Int.*, 2012, vol. 52, pp. 298–06.
13. S. Terasaki and K. Tsuzaki: *CAMP-ISIJ*, 2002, vol. 15, p. 1260.
14. Y. Matsumoto, K. Takai, M. Ichiba, T. Suzuki, T. Okamura, and S. Mizoguch: *ISIJ Int.*, 2013, vol. 53, pp. 714–22.
15. Y.H. Kim and J.W. Morris: *Metall. Trans. A*, 1983, vol. 14A, pp. 1883–88.
16. M. Gao and R.P. Wei: *Acta Metall.*, 1984, vol. 32, pp. 2115–24.
17. A. Shibata, H. Takahashi, and N. Tsuji: *ISIJ Int.*, 2012, vol. 52, pp. 208–12.
18. C.J. McMahon: *Eng. Fract. Mech.*, 2001, vol. 68, pp. 773–88.
19. P. Novak, R. Yuan, B.P. Somerday, P. Sofronis, and R.O. Ritchie: *J. Mech. Phy. Solids*, 2010, vol. 58, pp. 206–26.
20. M. Ichiba, K. Takai, and J. Sakai: *ISIJ Int.*, 2016, vol. 56, pp. 397–404.
21. C. San Marhi, T. Michler, K.A. Nibur, and B.P. Somerday: *Int. J. Hydrogen Energy*, 2010, vol. 35, pp. 9736–45.
22. J.A. Donovan: *Metall. Trans. A*, 1976, vol. 7A, pp. 1677–83.
23. H. Shoda, H. Suzuki, K. Takai, and Y. Hagihara: *ISIJ Int.*, 2010, vol. 50, pp. 115–23.
24. K. Takai, H. Shoda, H. Suzuki, and M. Nagumo: *Acta Mater.*, 2008, vol. 56, pp. 5158–67.
25. K. Sakaki, T. Kawase, M. Hirato, M. Mizumo, H. Araki, Y. Shirai, and M. Nagumo: *Scripta Mater.*, 2006, vol. 55, pp. 1031–34.
26. R. Gopaliengar, J.P. Wallace, and R.A. Oriani: *Mater. Sci. Eng.*, 1985, vol. 68, pp. 191–96.
27. A. Vehanen, P. Hautojärvi, J. Johansson, J. Yli-Kauppila, and P. Moser: *Phys. Rev. B*, 1982, vol. 25, pp. 762–80.
28. T. Doshida, H. Suzuki, K. Takai, N. Oshima, and T. Hirade: *ISIJ Int.*, 2012, vol. 52, pp. 198–207.
29. M. Hatano, M. Fujinami, K. Arai, H. Fujii, and M. Nagumo: *Acta Mater.*, 2014, vol. 67, pp. 342–53.
30. O. Madelen, I. Todoshchenko, Y. Yagodzinskyy, T. Saukkonen, and H. Hänninen: *Metall. Mater. Trans. A*, 2014, vol. 45A, pp. 4742–47.
31. T. Doshida, M. Nakamura, H. Saito, T. Sawada, and K. Takai: *Acta Mater.*, 2013, vol. 61, pp. 7755–66.
32. H.K. Birnbaum and P. Sofronis: *Mater. Sic. Eng. A*, 1994, vol. A176, pp. 191–202.
33. P. Sofronis and H.K. Birunbaum: *J. Mech. Phys. Solids*, 1995, vol. 43, pp. 49–90.
34. I.M. Robertson: *Eng. Fract. Mech.*, 2001, vol. 68, pp. 671–92.
35. T. Tabata and H.K. Birumbaum: *Scripta Metall.*, 1984, vol. 18, pp. 231–36.
36. A. Nagao, C.D. Smith, M. Dadfarnia, P. Sofronis, and I.M. Robertson: *Acta Mater.*, 2012, vol. 60, pp. 5182–89.
37. M.L. Martin, J.A. Fenske, G.S. Liu, P. Sofronis, and I.M. Robertson: *Acta Mater.*, 2011, vol. 59, pp. 1601–06.